# PACCSAP Wind-wave Climate: High resolution wind-wave climate and projections of change in the Pacific region for coastal hazard assessments

Claire E. Trenham, Mark A. Hemer, Tom H. Durrant and Diana J.M. Greenslade

CAWCR Technical Report No. 068

June 2013
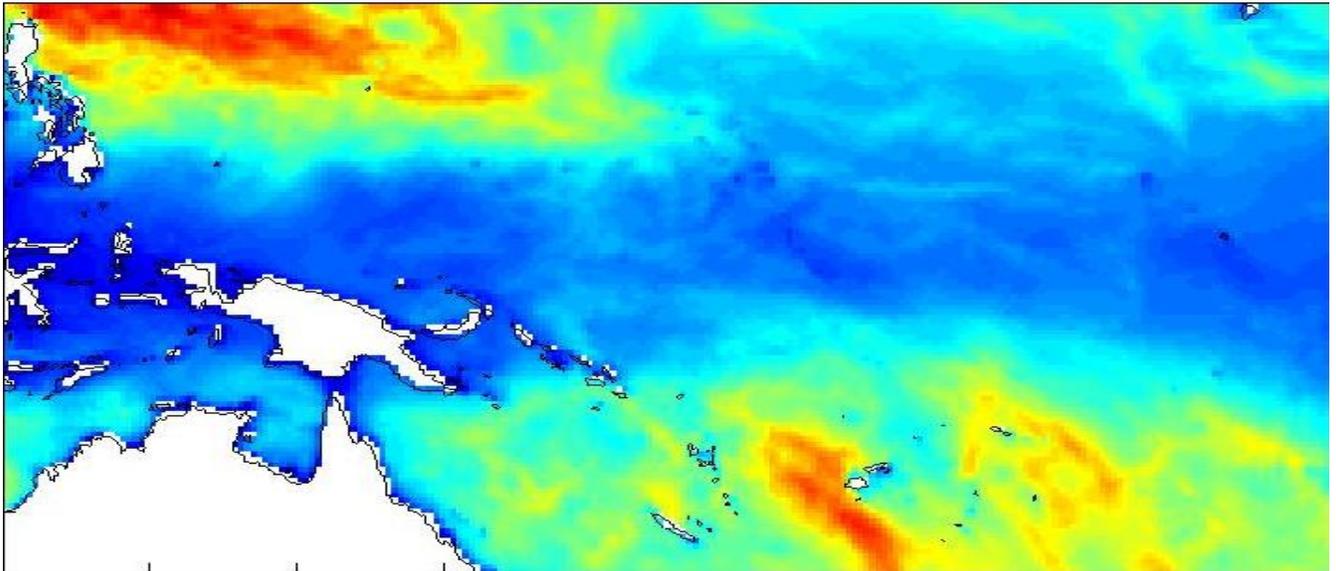
www.cawcr.gov.au

PACCSAP Wind-wave Climate: High resolution wind-wave climate and projections of change in the Pacific region for coastal hazard assessments

Trenham, C.E. [1], Hemer, M.A. [1], Durrant, T.H. [2] and Greenslade, D.J.M.[2]

[1] *Centre for Australian Weather and Climate Research – CSIRO, GPO Box 1538, Hobart, Tas 7001*
[2] *Centre for Australian Weather and Climate Research – Bureau of Meteorology, GPO Box 1289, Melbourne, Vic 3001*

Enquiries should be addressed to:
Mark Hemer
Centre for Australian Weather and Climate Research:
A partnership between the Bureau of Meteorology and CSIRO
GPO Box 1538, Hobart
Tasmania 7001, Australia

Mark.Hemer@csiro.au

Copyright and Disclaimer

All images reproduced in grayscale. A colour version of CAWCR Technical Report No.068 is available online: http://www.cawcr.gov.au/publications/technicalreports.php

Contents

List of Figures

List of Tables

EXECUTIVE SUMMARY

Surface wind-wave driven processes can impact on many aspects of Pacific Island coastal environments, and their climatological variability must be considered within any comprehensive assessment of potential climate change driven impacts on the coastal zone. These wave driven impacts include: coastal flooding during storm wave events; coastal erosion, both during episodic storm events and due to long-term changes in mean wave climate; characterisation of reef morphology and marine habitat/species distribution; flushing and circulation of lagoons; and potential shipping and renewable wave energy solutions.

As part of the Pacific-Australia Climate Change Science and Adaptation Planning (PACCSAP) Phase 1 program, we have contributed information about wind-wave climate in the Pacific, following on from our work in the Pacific Adaptation Strategy Assistance Program (PASAP) (Hemer, Katzfey and Hotan, 2011). Our contribution to PACCSAP Phase 1 comprised two aspects: a high resolution global and regional wave hindcast (Durrant, Greenslade, Hemer and Trenham, In prep), and climate model-driven projections of possible future wave climate. These data have been analysed for each Pacific Island Country and summarised in the "Update to Country Reports"[1].

Historical wave climate from hindcast

Observational wave data in the Pacific are sparse. A number of wave buoy records exist, however these are intermittent, and short lived. Continuous satellite altimeter coverage has existed since 1993; however the temporal and spatial characteristics of these data present a number of challenges on climate scales. Therefore modelled data are required to fill in the gaps in the observational datasets.

Numerical models provide a valuable supplement to observations. When forced with accurate winds, modern third generation spectral wave models have been shown by many studies to produce very accurate estimates of the wave field. By running these models using highly accurate atmospheric reanalysis data, it is possible to produce a high quality wave hindcast; an homogeneous dataset in both space and time with which to study wave climate.

Existing wave hindcasts and reanalyses in the Pacific region were examined (Hemer, Katzfey, and Hotan, 2011) and found to be too coarse both spatially and temporally to adequately capture the complex wave environment in the Pacific region. The lack of a high resolution wave hindcast has historically been limited by a lack of a suitably high resolution wind field with which to force a wave model. The recently completed NCEP Climate Forecast System Reanalysis (CFSR; Saha, et al., 2010) addresses this, delivering hourly surface winds on a 0.3 degree spatial grid, thus providing an opportunity to produce a significantly higher resolution wave hindcast than has previously been possible.

The NCEP CFSR surface wind dataset was used to force the WAVEWATCH III (WW3) wave model (Tolman, 1991; Tolman, 2009) from 1979 to the end of 2009 to generate a new high resolution hindcast (Durrant, Greenslade, Hemer and Trenham, In prep; Durrant, Hemer, Trenham and Greenslade, 2013).

---

[1] To be made available online at
http://www.pacificclimatechangescience.org/publications/reports/

Wave climate statistics were extracted from this hindcast for Pacific Island countries. The mean wave climate in the region was found to have a number of dominant features:

- Northerly swell contributions occurring in December-March from North Pacific extra-tropical storms.

- Southern Ocean generated swell is present year round, peaking in June-September.

- Locally generated trade wind waves typically peak in the winter of the respective hemisphere, but are affected by movement of the ITCZ and SPCZ.

- The West Pacific Monsoon can produce locally generated westerly waves in the western Pacific.

- Many locations observe extreme waves due to tropical cyclones.

- Interannual variability is frequently linked to the El Niño Southern Oscillation (ENSO), which can affect movement of the ITCZ and location of tropical cyclones.

- The Southern Annular Mode (SAM) can also affect interannual variability, particularly in the southern part of the region.

Model projections

Projected scenarios of how waves may be characterised in future time slices may be generated using dynamical wave modelling approaches in order to study possible wave climate change over the 21st century. Dynamical wave climate projections were carried out for a limited set of climate models, extending the work of (Hemer, Katzfey and Hotan, 2011).

Projections of future wave climates were made using 3-hourly surface wind data from selected CMIP5 climate models (HadGEM2-ES, INMCM4, CNRM-CM5 and ACCESS1.0), to drive the WAVEWATCH III wave model on a 1 degree grid between -80°S and 80°N. The four CMIP5 models were chosen due to their relatively high spatial resolutions, and early availability of high temporal resolution (3-hourly) data. The four models' monthly surface winds were compared to the full distribution of CMIP5 models' winds, and it was found that all four fall in the central two quartiles of projected winds. Thus these four models are typical of other CMIP5 models, but they do not represent the distribution of a full CMIP5 ensemble, although we assume they do in this analysis.

Wave projections were made for two future representative concentration pathways (van Vuuren, Edmonds, Kainuma, Riahi and Weyant, 2011), (medium-low emission RCP4.5 and high emission RCP8.5), over two 20-year periods (2026-2045 and 2081-2100), relative to a 1986-2005 historical period for each CMIP5 model.

To obtain projected changes in the wind-wave climate, the ensemble average of changes between each model's future scenario and historical baseline values was calculated.

Comparing the historical GCM simulations to the hindcast, substantial bias in the wave parameters was noted. The bias in wave properties of the historical GCM simulations from the hindcast dataset is typically larger than the changes between the historical and projection runs, which combined with the uncertainty of ENSO and similar index projections, identifies a caveat of uncertainty of the wave projections, with all wave projections having "low" confidence ratings.

The wave projections show an increased contribution of swell waves generated at the higher latitudes, particularly from the Southern Ocean, and reduced influence of easterly trade wind generated waves. Some changes in significant wave height[2], mean period and mean direction are projected to occur. In the western Pacific, a (sometimes statistically significant) decrease in wave heights and periods during the austral summer and a (statistically non-significant) increase in wave heights and periods during the austral winter is projected into the future with low confidence. Countries most likely to experience changes in wave climate include the Federated States of Micronesia, Fiji, Kiribati, Marshall Islands, Nauru, Palau, Papua New Guinea, Solomon Islands, Tuvalu and Vanuatu. These changes, accompanied with projected changes in wave direction should be considered within the context of long-term coastal response to physical drivers of change.

Wave climate projections carried out within this study suggest changes are anticipated over the 21st century under medium-low to high relative concentration pathways.

In summary, best estimates of projected changes in wave conditions over the next century include:

- Austral summer mean significant wave height is projected to decrease slightly in the western equatorial Pacific by approximately 0.2m (~5-10%), with greater decreases to the north of the equator.

- No statistically significant mean wave period change.

- Austral winter wave directions in the equatorial western Pacific display non-significant increasing southerly components associated with projected increases in Southern Ocean storms and easterly components associated with projected increases in trade wind strength. Trade winds are projected to decrease in strength somewhat in the boreal winter.

- Projected results are in agreement with those of Dobrynin, Murawsky and Yang (2012)

Data presented to partner countries

The wave model outputs give information on wave climate in terms of three main variables: Significant Wave Height (*m*), Mean Wave Period (*s*) and Mean Wave Direction (*degrees clockwise from North*). Data were averaged over two seasons, December-March and June-September, these data being tabulated. Mean annual cycles were also constructed for wave height and direction from the hindcast (Durrant, Greenslade, Hemer and Trenham, In prep), and wave height change from projections.

---

[2] Note that throughout this report, the term "wave height" refers to Significant Wave Height.

1   INTRODUCTION

1.1   Background to wave climate

The Earth's climate varies naturally over a range of time-scales - seasonal, inter-annual, decadal, centennial, and longer. These variations and trends drive a number of physical processes (e.g. sea level rise) which can impact on the coastal environment. These climate variations also drive changes in the atmospheric circulation, and consequently the surface winds. Surface wind generated waves (wind-waves) are generated by the action of wind on the sea surface, and as a result properties of wind-waves will vary in response to the variations in the surface atmospheric circulation. While the potential impacts of variability of wave climate can be large, until recently they have been mostly ignored. The Intergovernmental Panel for Climate Change (IPCC) fourth assessment report (AR4) noted that coastal impacts of climate change assessments focussed on sea-level rise, and suggested this be broadened to consider a larger number of coastal processes subject to climate variability and change (Nicholls, et al., 2007). Surface waves were identified as one of eight key drivers in the coastal zone requiring increased attention.

Wind generated ocean waves have a significant impact on coastal systems. Waves are generated by a forcing wind, but continue to travel away from the area of generation as swell. The observed wave field at any point therefore reflects both the locally generated waves (the wind sea) and waves which may have been generated a great distance away and travelled to that location (the swell). Thus, variability of the wind-wave climate at any location is not only a property of the local wind field, but the integrated variability of the wind field across large areas of the ocean over which the waves have been generated.

Modelling of deep water ocean waves around Pacific Island Countries allows an understanding of the wave climate, including Significant Wave Heights, wave periods (or lengths) and directions.

> *'Pacific Island Countries and Territories (PICTs) are arguably more vulnerable to variability and change in the surface wind-wave climate than sea-level rise. Future coastal vulnerability assessments for the region must consider potential changes in wave properties, together with the influence of mean sea-level rise and changes to other sea-level extremes.'* (Hemer, Katzfey and Hotan, 2011).

The coastal zone is affected, in part naturally, by sea level change, wind, waves, and storm surges. Sea level rise is a well-studied field, with projections of how the mean sea level may change in the Pacific in coming years being undertaken by (Church, White and Hunter, 2006; Zhang and Church, 2012). The effect of extreme sea levels from the contribution of waves, tides and pressure systems can be combined to make projections about coastal inundation during extreme events (Walsh, McInnes and McBride, 2012; Aucan, Hoeke and Merrifield, 2012). The main driver of storm surge in the Pacific is from tropical cyclones, several studies have looked into how they might change (Knutson, et al., 2010; Lavender and Walsh, 2011).

Thus an understanding of waves both in the current climate and in the future is important for present day and future extreme sea level modelling. The study of waves also has implications for coastal processes such as reef structure, distribution of marine species, lagoon circulation

and flushing, beach morphology, sediment transport, as well as implications for shipping routes and possible energy generation.

Throughout the tropical western Pacific, a multi-modal wave spectrum is observed, with contributions from locally trade wind generated seas, swell waves generated in both the northern and southern hemisphere extra-tropical storm belts, and episodic tropical cyclone events. The relative fraction of each of these components depends on location. Islands located on or north of the equator have wave fields dominated by the north-easterly trades and the northern Pacific generated swell, although Islands located further eastwards (e.g., Hawaii) also experience southern ocean swell. Islands located south of the equator have wave fields dominated by the south-easterly trades. Southern Pacific generated swell is also a major contributor to the wave climate in areas which are not sheltered by other islands (Hemer, Katzfey and Hotan, 2011).

Each mode of the Pacific wave climate varies seasonally and interannually, somewhat independent of each other. The North Pacific generated northerly swell waves peak in the boreal winter (around December-March), which leads to greater influence of this component of the wave field on most of the Northern Pacific during this period of the year. The Southern Ocean generated southerly swell waves are more consistent than the Northerly swell, but seasonal variability is observed with peaks in energy during the austral winter (around June-September) when the southern extra-tropical storm belt moves northwards. The contribution of trade wind generated waves peaks during the respective winter (boreal winter for the northern hemisphere north-easterly trades and austral winter for the southern hemisphere south-easterly trades). In the Western Pacific, the seasonal variability in the position of the monsoon trough (over ~20°S in February to over ~40°N in August) further influences the wave climate in this region, including the occurrence of tropical cyclone driven waves.

The predominant pattern of interannual change in the Pacific wave climate is associated with the El Niño Southern Oscillation (ENSO). The eastward shift in tropical cyclone activity during El Niño years leads to increases in wave height over large portions of the equatorial Pacific. Associated directional changes correlated with the Southern Oscillation Index (SOI) are also observed. Interannual variability of swell generated in the southern ocean is associated with variability of the Southern Annular Mode (SAM). High SAM Index values are associated with intensified Southern Ocean storm activity. During positive phases of the SAM, a wave height increase and greater southerly component is observed over large regions of the Pacific Ocean.

1.2   Wave modelling

Ocean waves may be simulated by wave modelling software such as WAVEWATCH III or SWAN[3], with bathymetry, surface wind forcing, sea ice boundaries, and potentially surface elevation and currents used for model forcing. When forced with reanalysis winds, past wave conditions can be simulated. Similarly, dynamical projections of future wave conditions can be derived using surface wind outputs from atmosphere-ocean coupled general circulation models (AOGCMs), thereby allowing projections to be made about how the wind-wave climate may change in the future. Such studies have been conducted globally and regionally (Hemer, Katzfey and Trenham, 2013; Hemer, Wang, Weisse and Swail, 2012; Hemer, Fan, Mori, Semedo and Wang, 2013; Fan, Held and Lin, 2013; Semedo, Weisse, Behrens, Sterl, Bengtsson and Günther, 2013; Mori, Shimura, Yasuda and Mase, 2013), and with an emphasis on the Pacific region (Hanson, Tracy, Tolman and Scott, 2009; Hemer, Katzfey and Hotan, 2011).

---

[3] http://www.swan.tudelft.nl/

Available long-term wave data for the Pacific region have been compiled (Hemer, Katzfey and Hotan, 2011), including available in situ wave buoy records, model hindcast and reanalyses products, and satellite altimeter derived records. Observed wind wave data from buoys are spatially sparse and temporally limited in the Pacific, consequently the data contain little information to identify the key modes of inter-annual (and decadal) wave climate variability, and little of the data contains directional information. Satellite altimeter data exist since 1993 and provide a useful data set (Young, Zieger and Babanin, 2011), however this too is spatially and temporally limited, has a long sampling interval at any point, and no directional information. Thus it is useful to complement the observations with modelled hindcast or reanalysis wave data e.g. Dee et al. (2011). Hindcasts produced from numerical models provide a homogenous data set in both space and time with which to study long term wave climate.

Existing wave hindcasts in the Pacific region were examined by Hemer, Katzfey and Hotan (2011) and found to be too coarse both spatially (around 1.5°) and temporally (around 6-hours) to adequately capture the complex wave environment in the region of interest, which highlighted the need for a high-resolution hindcast. The ability to produce such a hindcast has previously been limited by the lack of a global high resolution reanalysis wind product with which to force the wave model. The recently completed Climate Forecast System Reanalysis (CFSR; Saha, et al., 2010), performed at the National Centers for Environmental Prediction (NCEP), provides such a product. Surface winds are available from this reanalysis hourly on a global 0.3 degree spatial grid, providing an opportunity to produce a significantly higher resolution wave hindcast, particularly in the Pacific region, than has previously been possible.

The NCEP CFSR surface wind data were used to force the WAVEWATCH III (WW3) wave model (Tolman, 1991; Tolman, 2009) from 1979 to the end of 2009 to generate a new high resolution hindcast (Durrant, Greenslade, Hemer and Trenham, In prep). This hindcast comprised three levels of resolution – a 0.4 degree global grid providing two-way nested boundary data to high resolution subgrids of 10 and then 4 arcminutes around Australia and Pacific Island countries (Fig. 1) (Durrant, Hemer, Trenham and Greenslade, 2013). All output data were archived at hourly intervals. Details of the hindcast performed and used in this study can be found in Durrant et al. (In prep), including verification against observational data.
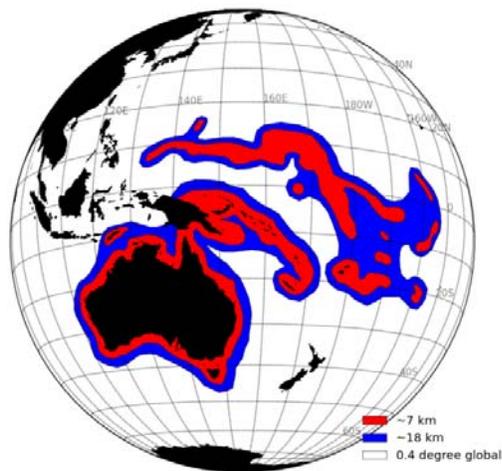
Fig. 1 Region of 30-year high resolution "CAWCR wave hindcast", showing a global 0.4 degree grid (white) with a series of nested grids of 10 (blue) and 4 (red) arcminutes (~18 and ~7km respectively).

The use of wave models is advantageous in producing spatially homogeneous datasets, which can in the future also be used to drive finer scale models through nested grids. Furthermore, through hindcast modelling a comparison with observed data can be made, and comparison with the historical GCM simulations can identify uncertainties in model values and projections of future changes in wave climate.

Projecting future change in Pacific wave climate is in part dependent on the climate models' ability to represent sources of interannual variability in waves, such as that due to ENSO. Most (but not all) previous generation CMIP3 climate models were qualitatively consistent in their projections of mean changes over the tropical Pacific (warming sea surface temperature (SST) and general weakening of the Walker Circulation) (Guilyardi, et al., 2009). However, these models are inconsistent with respect to their projections of change in ENSO variability (some models show increasing ENSO variability, others exhibit no change, others show a decrease).

Wave climate projections for the Pacific Ocean will benefit from future improvements in ENSO model skill. Early analysis of the CMIP5 climate model ensemble suggests that the caution with such projections that was needed with CMIP3 models is still required (Grose, et al., accepted). Furthermore, substantial differences can arise in the wave projections due to emissions scenarios, down-scaling methods and modelling approaches (Hemer, Fan, Mori, Semedo and Wang, 2013), which leads to low confidence in wave climate projections.

Figure 2 shows the region of interest for this work, containing the fifteen partner countries involved in the programme: Cook Islands, East Timor (Timor-Leste), Federated States of Micronesia (FSM), Fiji, Kiribati, Marshall Islands, Nauru, Niue, Palau, Papua New Guinea, Samoa, Solomon Islands, Tonga, Tuvalu and Vanuatu.
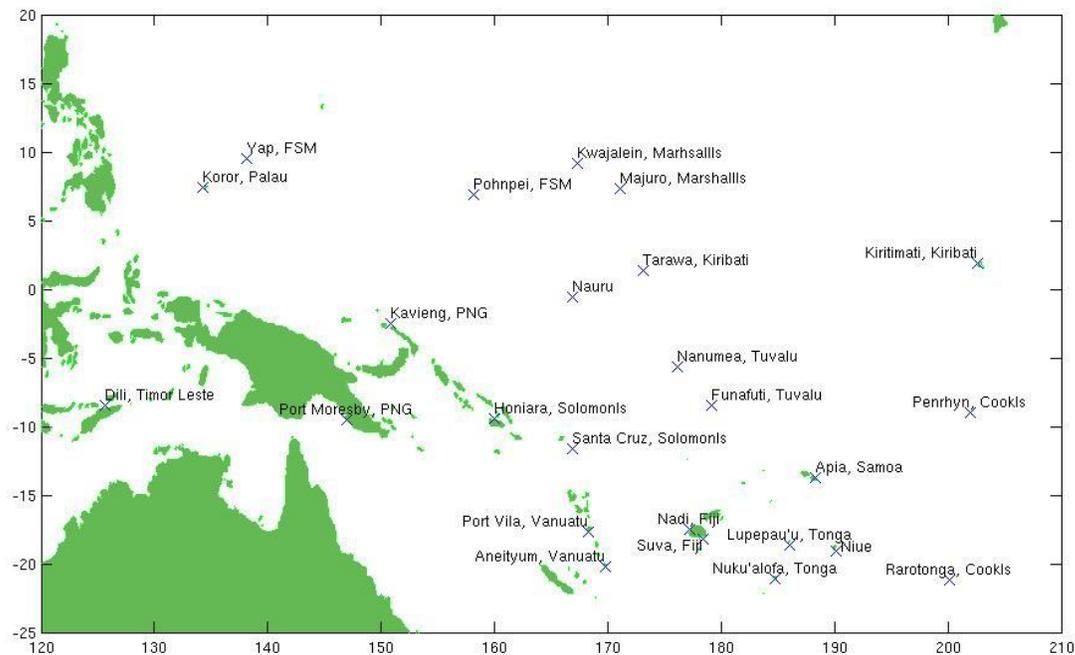
Fig. 2   Map of the Western Pacific, with crosses indicating the locations where wave data were extracted for analysis for each of 15 partner countries.

2   DATA PROCESSING METHODS

This study contained two major components, with similar modelling methods but different applications. The first is the wave hindcast, produced to give a fine scale description of the wave climate across the Pacific region. The second is a suite of climate model forced wave simulations on a coarser grid than the hindcast, used to make country-scale projections about wave climate.

WAVEWATCH III (Tolman, 1991; Tolman, 2009) was used as the wave modelling software for this project. An overview of the modelling procedures is shown in Fig. 3. We derive our description of the current wave climate directly from the hindcast (see Section 2.1 and Section 3). Projections are made by running the wave model using the "historical" climate model output, and also future scenario model outputs. The projected change in wave climate is the difference between these values, for each future time slice and emissions scenario (see Section 2.2 and Section 4).
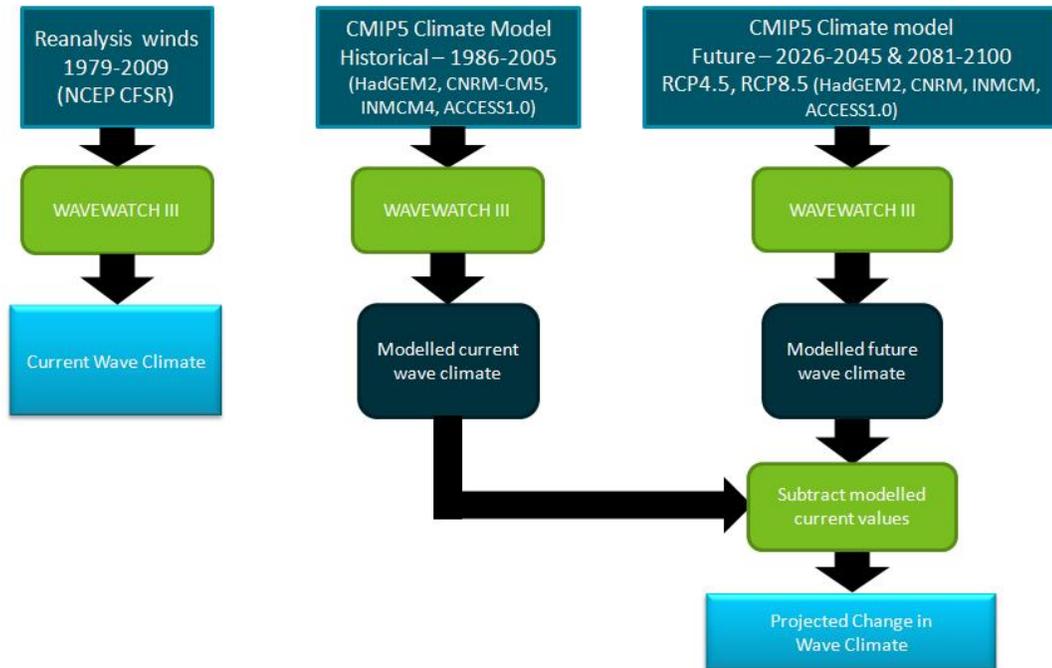
Fig. 3 Wave climate description in the present context is developed from a hindcast made by forcing a wave model with reanalysis winds (left), while projected changes are estimated by forcing the wave model with CMIP5 model winds and looking at the changes in wave properties between historical and future time slices (right).

2.1 Wave hindcast

As described previously, existing observational wave data products are of insufficient duration and/or resolution to provide useful descriptions of the current wave climate for PICs. The previous best wave hindcast data product available did not have sufficiently fine spatial or temporal resolution for our studies, thus a higher resolution hindcast using nested grids around islands of interest to this project was undertaken to address this.

The hindcast was run from 1979-2009 using the WAVEWATCH III™ model version 4.08 (Tolman, 1991; Tolman, 2009). A series of nested grids were run within a global grid, following the so called mosaic grid approach of (Tolman, 2008). This framework enables a series of overlapping grids of different resolutions to be run simultaneously, with fine scale grids receiving information from coarse grids, and the added detail achievable in fine grids being fed back up to the coarse grids, enabling the model resolution to be locally increased while maintaining consistency between grids (see Fig. 1). All grids were forced with CFSR (Saha, et al., 2010) surface winds at 0.3° spatial and hourly temporal resolution. Six-hourly sea ice concentrations from the CFSR data set were used to define the ice edge. For further details see Durrant et al. (In prep).

2.1.1 Data Presented

The wave model outputs give information on wave climate in terms of a number of variables. In this report we are primarily interested in three main variables: Significant Wave Height (*m*),

Mean Wave Period (*s*) and Mean Wave Direction (*degrees clockwise from North*). Other variables were also computed and archived but are not discussed here.

Regional maps of bulk wave properties are presented. Specific wave distribution analysis was performed only at points of interest (e.g. capital cities) in the region, with data extracted from the nearest model grid point from the 4 arcminute hindcast. In Section 3.2.3 we have used the island nation of Nauru for the purposes of demonstration.

A mean climatological annual cycle for each variable was generated by finding the average of all values in each month over the dataset. Wave height and direction only were plotted in the Update to Country Reports, for brevity, while seasonal mean values and confidence ranges were given for all three variables, as described below. We also demonstrate the use of "wave roses" and radial probability distributions as alternative methods of visualisation for variables with directional attributes.

Seasonal Variability

When reporting typical values of wave parameters it is important to give a range of variability. In this project two times the standard deviation, 5-95% percentile intervals were the preferred method. For annual cycle data, the monthly mean was plotted, with a box drawn at 1 standard deviation from the mean, determined from all data in that month. Bar whiskers showed the 5th and 95th percentiles, giving an indication of interannual variability. 5-95th percentile values were also used to give numerical ranges in tabulated data over two four-month seasons, December-March and June-September (typically "wet" and "dry").

Storm and extreme values

In this study, "storm waves" were considered to be those with Significant Wave Heights above the 99th percentile value of the whole data set. Typical storm wave properties were found by examining the periods and directions of these large waves, as well as which months they occur.

Extreme value analysis was used to estimate the 1 in 50 year return wave height. Using Extreme Value Theory, the height of a wave with a 50 year return period was estimated by applying the Generalised Extreme Value distribution generated from monthly maximum wave heights over the period of the hindcast to estimate the maximum statistical wave height.

Note the predicted extreme values are underestimates due to not fully resolving tropical cyclones.

Interannual variability

In order to investigate interannual variability, we regressed our monthly mean wave data against the Southern Oscillation Index (associated with the El Niño/La Niña cycle, defined by the Troup SOI threshold) and the Southern Annular Mode Index, both of which may impact on the direction and strength of forcing winds in a given year. This is determined by calculating the wave power (wave energy flux, dependent on significant wave height, period, and direction), and plotting the mean wave power in each season according to index sign. Where there are substantial differences in mean wave properties between phases of the index, this dependence is noted in the Update to Country Report wave climate descriptions.

2.2 CMIP5 model-forced wave simulations

In preparation for the CMIP5 model runs, NCEP CFSR reanalysis wind data were used to force the wave model at 1 degree resolution, and some tuning runs were performed to adjust the physics to reduce the bias of wave height particularly in the Southern Ocean when compared to other reference data sets. WAVEWATCH III v3.14 was implemented with WAM4 physics (Bidlot, Janssen and Abdalla, 2005), with tuning parameter BETAMAX=1.25 (as opposed to 1.2) the only difference from default settings. These model settings were then used when applying CMIP5 wind forcing.

Projections of future wave climates were made using 3-hourly surface wind data from selected CMIP5 climate models (HadGEM2-EM, INMCM4, CNRM-CM5 and ACCESS1.0), to drive the WAVEWATCH III wave model on a 1 degree regular grid between -80˚S and 80˚N.

The four CMIP5 models used were chosen due to their relatively high spatial resolutions, and early availability of high temporal resolution (3-hourly) data (see Table 1). Projections were made for two future Representative Concentration Pathways (van Vuuren, Edmonds, Kainuma, Riahi and Weyant, 2011), medium emissions RCP4.5 and high emissions RCP8.5, over two 20-year periods (2026-2045 and 2081-2100), relative to a selected 20-year historical period, 1986-2005. The projected changes in wind-wave climate are the ensemble average of changes between each model's future scenario and its historical values (see Fig. 3).

Table 1 WAVEWATCH III model runs showing three time periods (historical and two future epochs), with future periods being studied for two CMIP5 RCP emissions scenarios. A comparison run on the same grid using CFSR wind forcing was also produced.

CMIP5 GCM	RESOLUTION	1979-2005	2026-2045	2081-2100
ACCESS1.0	N96L38 (~1.875° x 1.25°)	Historical, r1i1p1	RCP4.5, r1i1p1 RCP8.5, r1i1p1	RCP4.5, r1i1p1 RCP8.5, r1i1p1
CNRM-CM5	TL127L31 (~1.4°x1.4°)	Historical, r1i1p1	RCP4.5, r1i1p1 RCP8.5, r1i1p1	RCP4.5, r1i1p1 RCP8.5, r1i1p1
HadGEM2-ES	N96L38 (~1.875° x 1.25°)	Historical, r2i1p1	RCP4.5, r1i1p1 RCP8.5 r1i1p1	RCP4.5, r1i1p1 RCP8.5, r1i1p1
INMCM4	2° x 1.5°	Historical, r1i1p1	RCP4.5, r1i1p1 RCP8.5, r1i1p1	RCP4.5, r1i1p1 RCP8.5, r1i1p1
NCFSR	0.5° x 0.5°	Hourly forcing	-	-

2.2.1 Data Presented

Due to the coarse spatial resolution of the CMIP5 models, for most countries, a grid covering the area was extracted and averaged at each time step to make regional projections. For countries covering a wider area (such as Kiribati) more than one grid was used.
Projection data were analysed in a similar way to the historical hindcast data. While regional maps of overall change are produced for basic variables, here we have examined only specific country data; again using Nauru as an example in Section 4.1.2.

An annual cycle of the projected change in wave climate was generated by calculating the difference between the mean future time-slice data and the mean historical value in each month. For each of the four models, the average of all values in each month was calculated for each variable, in both historical and future data. The difference between each model's future and historical values was found for each month. The projected change in that month was the mean of the models' differences (see Fig.18 in Section 4). Wave height change was plotted in the Update to Country Reports, with seasonal mean values and confidence ranges given for all three variables.

Uncertainties

In handling uncertainty in plots, the ensemble mean difference was plotted (see above), with a box showing the standard deviation of the four models' differences in each month, assuming they are representative of the full CMIP5 spread. This is a very small sample so is likely to be an underestimate of the full range of CMIP5 model means (Hemer, Fan, Mori, Semedo and Wang, 2013). The 5-95% error bar range was estimated as 1.64 times the standard deviation of the model means. Assuming a normal distribution this represents a 90% range. In tabulating results, values were calculated seasonally (December-March and June-September) rather than

monthly, with uncertainty ranges representing the 5-95% range. The same method was used to calculate these confidence ranges, but using the standard deviation of the four models over each four month season (i.e. the standard deviation of sixteen values).

3 HISTORICAL WAVE CLIMATE

3.1 Background to hindcast

The hindcast described in Section 2.1 and in more detail in Durrant et al. (In prep) provides the basis on which current wave climate for each country is defined in this work. In addition to these derived country specific products, the hindcast itself provides a valuable resource for further research in the Pacific.

3.2 Data analysis and results

Wave climate descriptions were made for each of the locations shown in Fig.2. In this document we focus on the wave climate of Nauru, located at (0.53˚S, 166.93˚E), as an example.

3.2.1 Mean wave properties

The wave hindcast provides a significant reference data source for waves in the region. Figures 4 through 7 show mean significant wave height and mean wave direction over the typical extreme season periods of December-March (Figs 4 and 5) and June-September (Figs 6 and 7).

In many instances these two seasons may be classified as "wet" or "dry", depending on hemisphere and location.

In December-March (southern hemisphere tropical wet season), the largest waves are seen in the tropics (Fig. 4). These may be locally generated by trade winds, monsoon winds and tropical storm systems, while larger swell waves propagate southward from northern hemisphere winter storms in the North Pacific, with some swell influence from the South Pacific and Southern Ocean. Waves in the tropics are largely easterly and north-easterly due to northern hemisphere trade winds, with westerly monsoon waves visible in the Timor and Arafura Seas (Fig.5 December – March mean wave direction) Southerly and south-easterly waves dominate to the east of Australia.

Some of these propagating swell systems from storms are associated with inundation events on low-lying islands in the region (Harangozo, 1992; Aucan, Hoeke and Merrifield, 2012; Hoeke, McInnes, Kruger, McNaught, Hunter and Smithers, 2013).
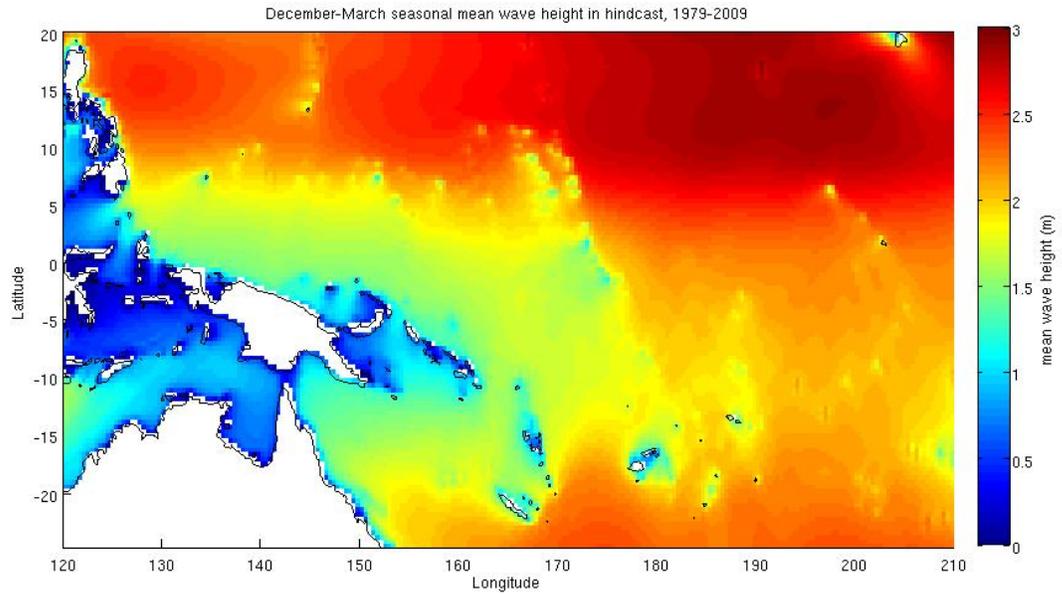
Fig. 4   December-March mean significant wave height.
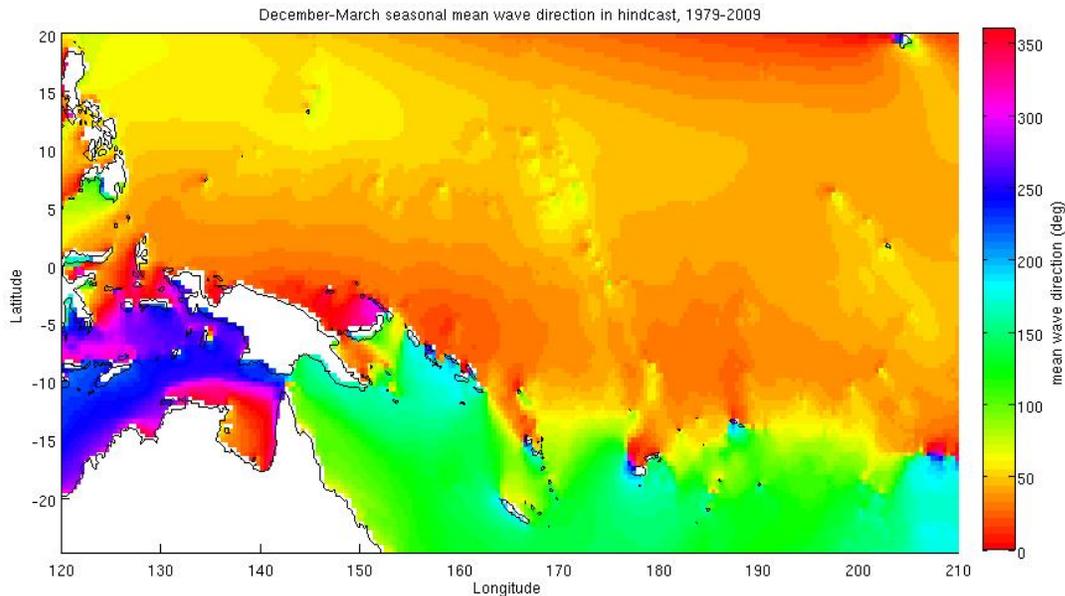
Fig. 5   December-March mean wave direction.

In June-September (northern hemisphere tropical wet season, southern mid-latitude storm season), the largest waves are those in the southern part of the region associated with winter winds in the south (Fig. 6). The eastern part of the tropical region also shows signs of larger trade wind-generated waves. Waves in this season may be locally generated by trade winds from the east or monsoon winds from the west, while larger swell waves propagate northward and northeast from winter storms in the southern oceans. Waves in the tropics are largely south-easterly due to southern hemisphere trade winds, with a monsoonal influence in the northwest (Fig. 7).
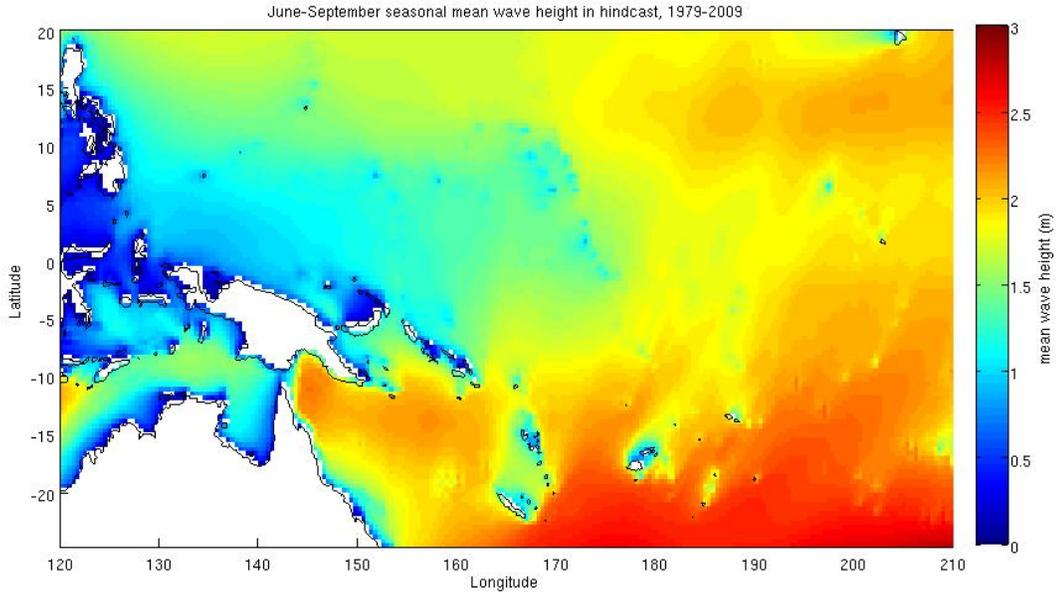
Fig. 6   June-September mean significant wave height.
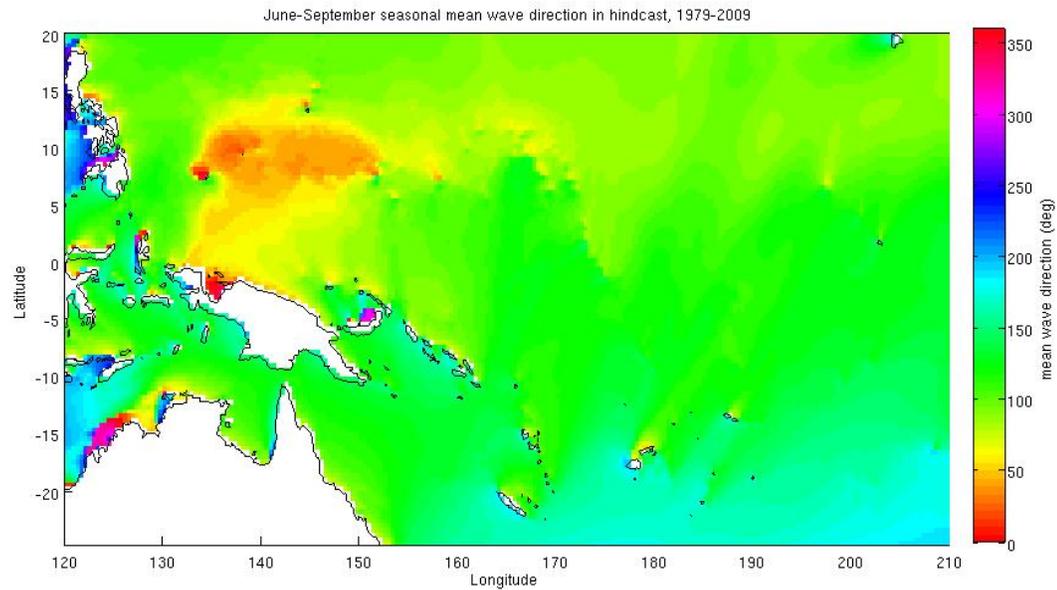
Fig. 7   June-September mean wave direction.

3.2.2 Storm and extreme wave events

Storm wave heights (99th percentile) have been calculated across the region (Fig.8). It can be seen that open regions away from the equator typically experience larger storm wave heights than at the equator due to the ITCZ and away from the sheltering effect of large islands. Many of the large wave heights are likely to be associated with tropical cyclones, though some may also result from propagation of large swell waves from storms at higher latitudes into this region.
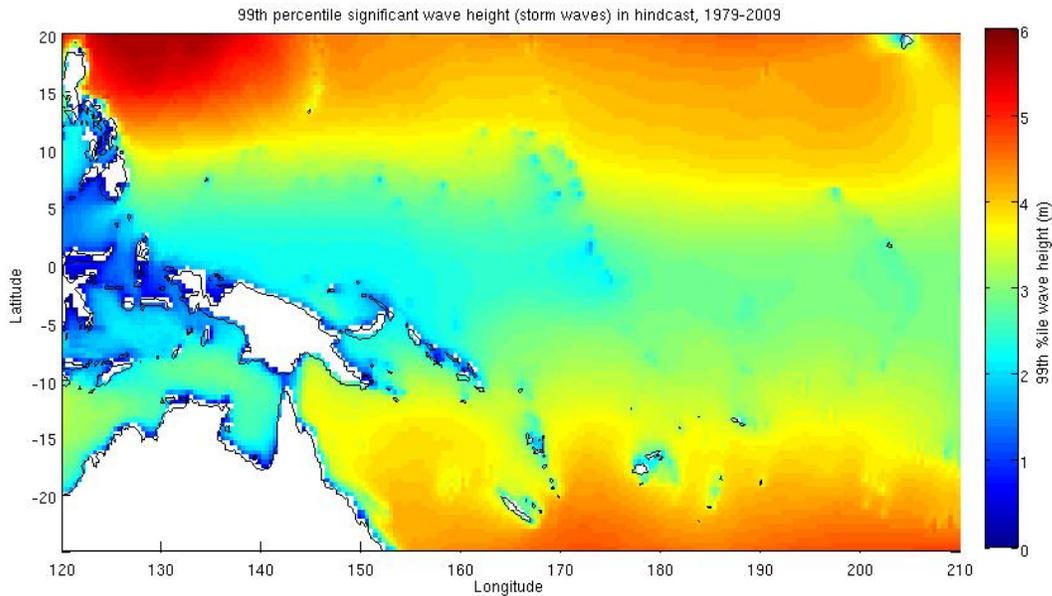
Fig. 8   99th percentile significant wave height, indicating the size of the largest storm waves (1% of waves).

Extreme wave height is defined here as the significant wave height of a 1-in-50 year wave event (Fig.9), calculated using Extreme Value Theory. The zone around the equator has relatively small extreme waves, although such waves could nevertheless potentially be highly damaging to the islands in the region. Further away from the equator, we see the possible occurrence of very large waves, which would likely occur during tropical cyclones or typhoons.
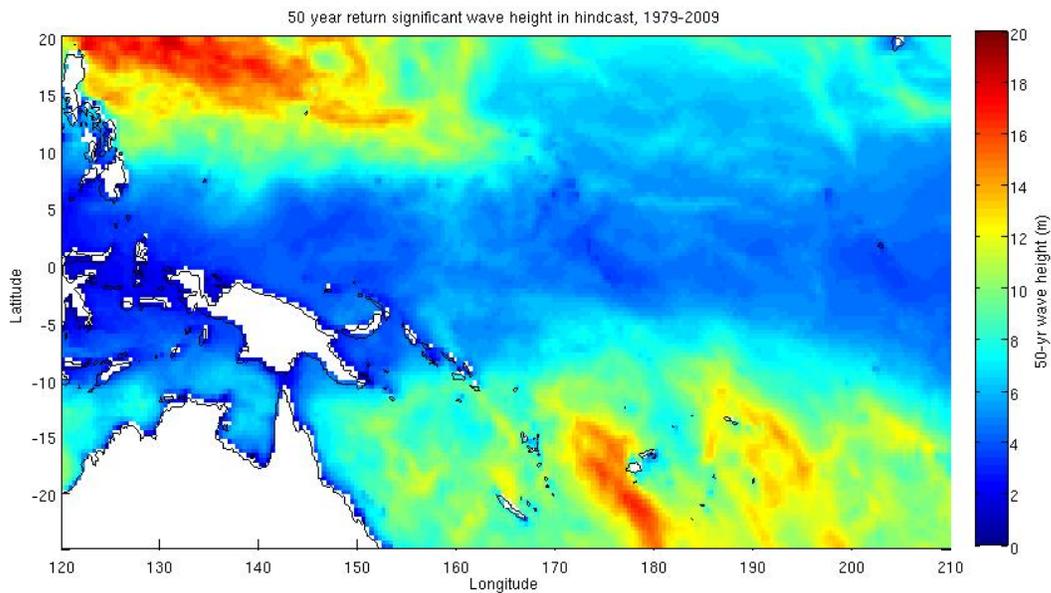
Fig. 9   Height of waves with a 50 year return period, based on the hindcast data.

3.2.3 Country example – Nauru

The Update to Country Reports provide a description of the wave climate for each of fifteen partner countries. Here we present an example of the wave climate description, as well as some further plots for the island nation of Nauru.

Figure 10 shows annual cycles of the wave variables significant wave height (blue) and mean wave direction (green) as described in Section 2.1.1.
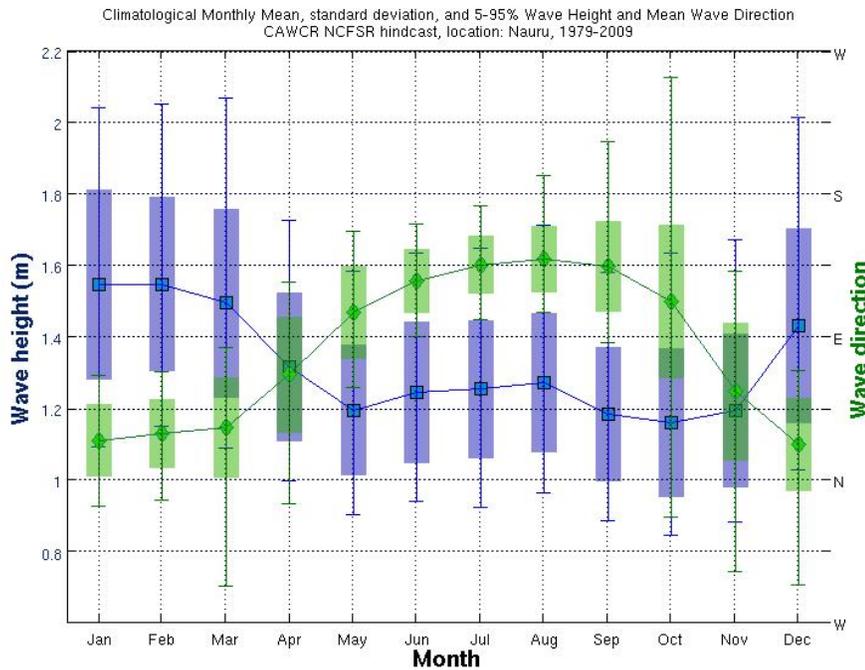
Fig. 10   Annual cycle of wave height (blue) and mean wave direction (green) at Nauru.

The wind-wave climate of Nauru is strongly characterised by the seasonal trade winds. On the west coast of Nauru, waves are directed from the south-east due to southern hemisphere trade winds during the dry season (June-September) and are typically smaller than in other months, with swell waves incident from the south resulting from extra-tropical storms. Waves are directed on average from the north-northeast, and are typically larger than in other months during the wet season (December-March), comprising locally generated northern hemisphere trade wind waves, as well as westerly wind waves due to monsoon systems and northerly swell from North Pacific extra-tropical storms. Wave period does not vary significantly throughout the year (not shown).

We also present seasonal data in tabular form for this location (Table 2). Here we give values for the three variables of interest averaged across the wet and dry seasons (December-March and June-September respectively) for both the hindcast and the historical GCM models. The historical runs model June-September wave heights well at this location but over-predict the December-March wave heights by ~20cm, suggesting an enhanced seasonal cycle in the simulations, and indicating some model bias may be present.

The differences between the hindcast values and the CMIP5 model ensemble average values may be due to different input winds and different model physics. They may also be an artefact

of the different grid resolutions used. Some of the differences can be assessed by comparing the global hindcast to a wave model run with CFSR wind forcing on the same grid as the CMIP5 models. The magnitude, direction and timing of bias between models and the hindcast varies across the region. There is a positive bias in wave height (~0.2m) in the central area of the region at the higher resolution in December-March, with positive bias in the west and negative in the east in June-September. However, there is a substantial negative difference near islands where many of the locations of interest lie, suggesting the hindcast may produce much smaller reported wave heights than the coarser models. This may account for some apparent overestimation of wave height by the climate models. Wave direction also varies between the two CFSR-forced models. These differences are likely to be a combination of the higher grid resolution of the hindcast, which is more capable of resolving islands, and the different model physics used in the hindcast than the 1 degree runs, which in particular affects swell dissipation. At Nauru, the climate models overestimate wave height for most of the year compared to the hindcast, with less bias in the dry season (June-September).

Table 2 **Seasonal wave data with 5-95% values near Nauru showing significant wave height, mean wave period and mean wave direction in December-March and June-September, for both the hindcast (observation) data and the climate model simulations ensemble. A compass relating number of degrees to cardinal direction is shown.**
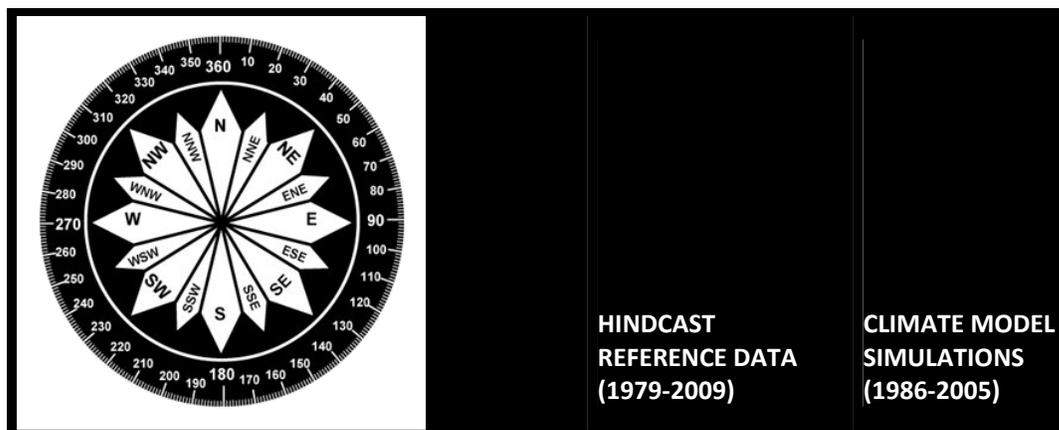
		HINDCAST REFERENCE DATA (1979-2009)	CLIMATE MODEL SIMULATIONS (1986-2005)
Mean wave height (m)	**December-March**	1.5 (1.1 – 2.0)	1.7 (1.4 – 2.0)
	June-September	1.2 (0.9 – 1.7)	1.2 (1.1 – 1.4)
Mean wave period (s)	**December-March**	9.3 (7.5 – 11.6)	8.4 (7.5 – 9.7)
	June-September	8.6 (7.0 – 10.3)	7.9 (7.1 – 8.6)
Mean wave direction (˚ clockwise from North)	**December-March**	30 (320 – 70)	40 (20 – 60)
	June-September	130 (100 – 180)	120 (100 – 140)

 "Wave roses" can also be used to visualise the data, giving the probability of wave events occurring as distance from the centre of a circle. Wave direction is indicated by the angle and wave height by colour.

In addition to integrated wave parameters for the full spectrum, the hindcast outputs also included those for four spectral partitions, calculated following (Hanson and Phillips, 2001). This allows investigation of locally generated wind sea independently from remotely generated

swell. Figure 11 comprises four wave roses, two for each season. The top pair of wave roses shows the locally generated wind-sea conditions, while the lower pair is taken from the first spectral partition and represents the dominant swell component.

In Fig.11 we see that in the wet season the majority of locally generated wind-sea waves (top left panel) come from between the north and east due to northern trade winds; however the very small number of waves generated in the west can have greater wave heights. At this time of year, swell waves (bottom left panel) come from the north and northeast due typically to extra-tropical storms. In the dry season, the majority of locally generated wind-sea waves (top right panel) are from the northeast and southeast due to trade winds, with the largest of these waves being generated in the east and east-southeast. Most swell waves (bottom right panel), meanwhile, come from the south and southeast due to storm waves propagating northwards from the Southern Ocean.

These plots are consistent with the data shown in the annual cycles (Fig.10), and this may be considered an alternate visualisation for seasonal, rather than monthly, data.
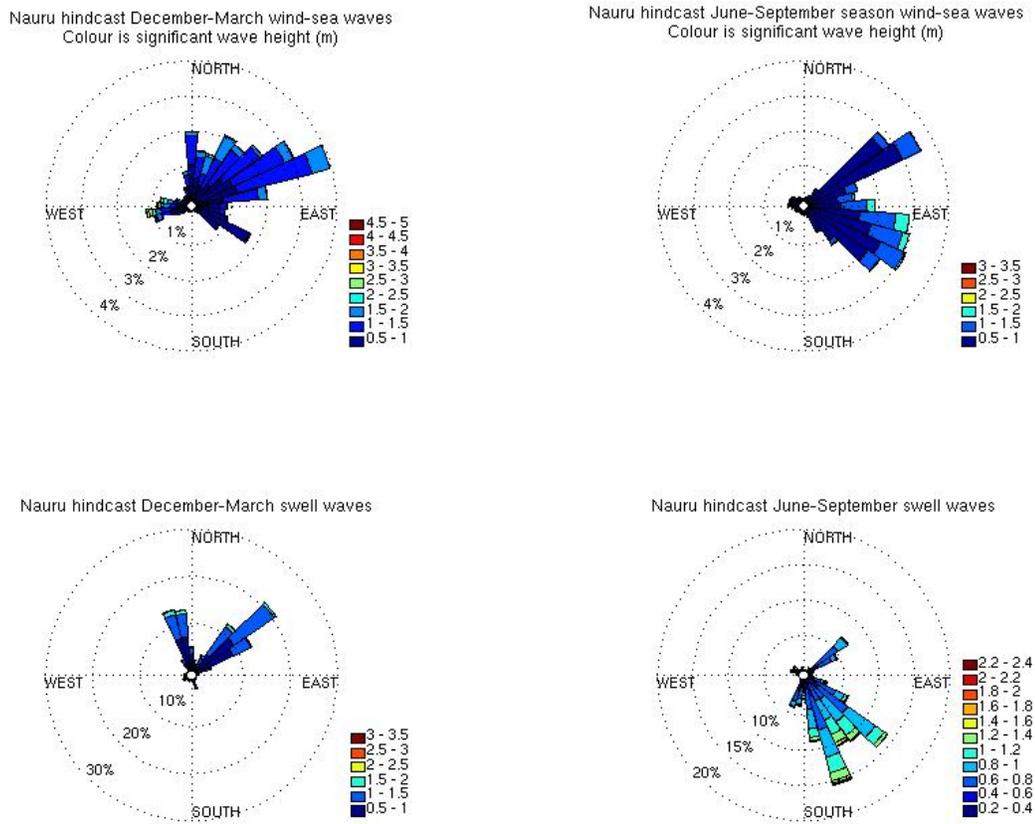
Fig. 11 Wave roses showing the probability of wave heights as a function of their source direction in the wet season (left) and dry season (right), with locally generated wind waves (top panels) and remotely generated swell waves (lower panels).

Figure 12 demonstrates another way of presenting the data. This shows a radial bivariate probability distribution, comparing mean wave period (distance from centre) to mean wave direction (angle), where colour denotes the probability of a wave with those parameter values occurring. In the wet season, December-March (Fig. 12 left), waves are incident from the west through to just south of east, with the majority originating from the northeast. In the dry season,

June-September (Fig.12 right), waves range from east through to southwest, with the majority of waves directed from the southeast. There are more waves of shorter period in June-September than in December-March.
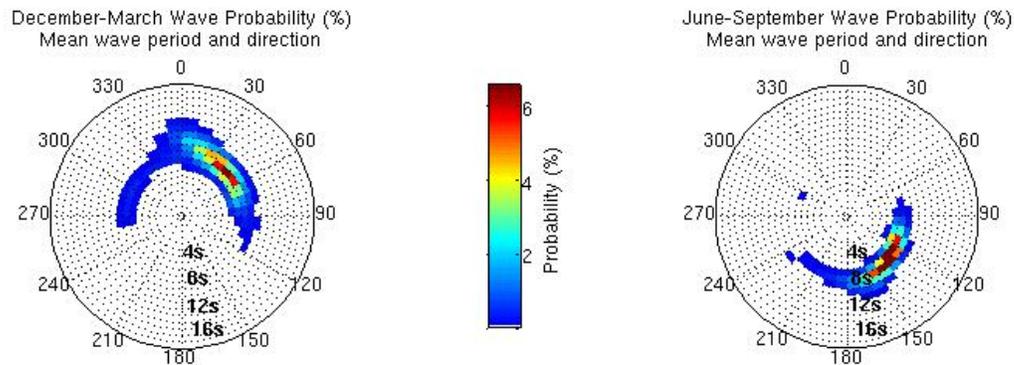
Fig. 12   Radial bivariate probability distribution of mean wave direction and mean wave period in the wet season (left) and dry season (right).

Storm and extreme wave events

At Nauru, storm waves larger than 2.3m (99th percentile) occur predominantly during the wet season, generated by the boreal winter North Pacific extra-tropical storms and are observed as long, northerly and north-westerly swell. Some large westerly waves, likely to be generated by Tropical Cyclones near the Philippines based on their wavelength and direction, have been observed in other months (August and November). The height of a 1-in-50-year wave event on the west coast of Nauru is calculated to be 5.0m.

Interannual variability

No suitable observations are available to assess long-term historical trends across most of the Pacific. However, inter-annual variability may be assessed in the hindcast record by comparing the data to climate indices such as the SOI (Southern Oscillation Index) and SAMI (Southern Annular Mode Index).

The wind-wave climate displays strong inter-annual variability at Nauru, varying strongly with ENSO (El Niño/Southern Oscillation). During La Niña years, wave power is approximately 30% greater than during El Niño years in the wet season (December-March), and waves are more strongly directed from the east year round, associated with increased trade wind speeds. At Nauru, no correlation is observed with the Southern Annular Mode.

4 CMIP5 CLIMATE MODEL-FORCED WAVE SIMULATION: WAVE CLIMATE PROJECTIONS

The monthly surface winds of the four models used (HadGEM2-ES, CNRM-CM5, INMCM4, ACCESS1.0) were compared to the full distribution of CMIP5 monthly model winds, and it was found that all four fall in the central two quartiles of projected winds. Thus these four models are considered to be typical of other CMIP5 models representing some spread in ensemble uncertainty, however the exact range of 60 CMIP5 future projections is larger than the modelled range presented.

The WW3 wave model was driven by 3-hourly GCM surface winds and monthly sea ice coverage with outputs saved every six hours, and monthly averages calculated from the output data.

Comparing the historical GCM simulations to the hindcast, substantial bias in the wave parameters was found. The bias in wave properties of the GCM simulations from the hindcast dataset is typically larger than the changes between the historical and projection runs (Table 3, also see Table 2), which when combined with the uncertainty of ENSO index and similar projections, identifies a caveat of uncertainty of the wave projections, implying low confidence ratings (Hemer, Fan, Mori, Semedo and Wang, 2013). Note that the GCM simulations are run at $1°$ grid resolution, much lower than the available hindcast resolution.

4.1 Data analysis and results

4.1.1 Mean wave properties

In this subsection we consider only the scenario of greatest projected change in the region, that is, we look at the difference between the historical models and the last 20 years of the 21st century under a high emission RCP8.5 scenario.

Figures 13 through to 16 show the average difference in significant wave height and mean wave direction between future and present models in December-March and June-September. A substantial decrease in wave height across much of the region in December-March (Fig. 13) is indicated (up to 10%) particularly to the north of the equator, while little change is projected in wave direction (Fig. 14), with clockwise rotations around some South Pacific islands, an anticlockwise change in the northeast of the region, and rotations around French Polynesia (far east of plot) to be more easterly. In June-September (Fig. 15) little change is projected, with a slight increase in wave height across much of the southern part of the region; a clockwise rotation is projected in the northern part of the region (Fig. 16) (a greater contribution of the southerly component of the wave field), while in the southern part of the region a slight anticlockwise rotation with a stronger southerly component is projected. These Figures indicate a possible decrease in driving winds in December-March, while in June-September a strengthening in southern hemisphere trade winds may produce a clockwise rotation in the northern tropics. There is also a suggestion of increased southerly swell from extra-tropical storms in the Southern Ocean and South Pacific. These results are in agreement with those of Dobrynin, Murawsky and Yang (2012) who presented CMIP5 based projections.
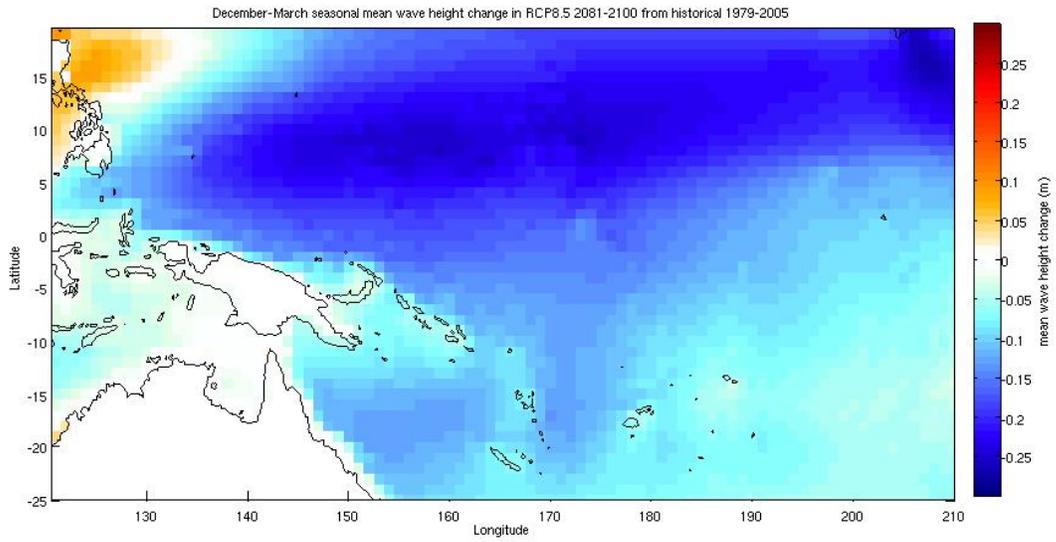
Fig. 13 December-March projected change in mean wave height from historical (1979-2005) values in 2081-2100 under RCP8.5.
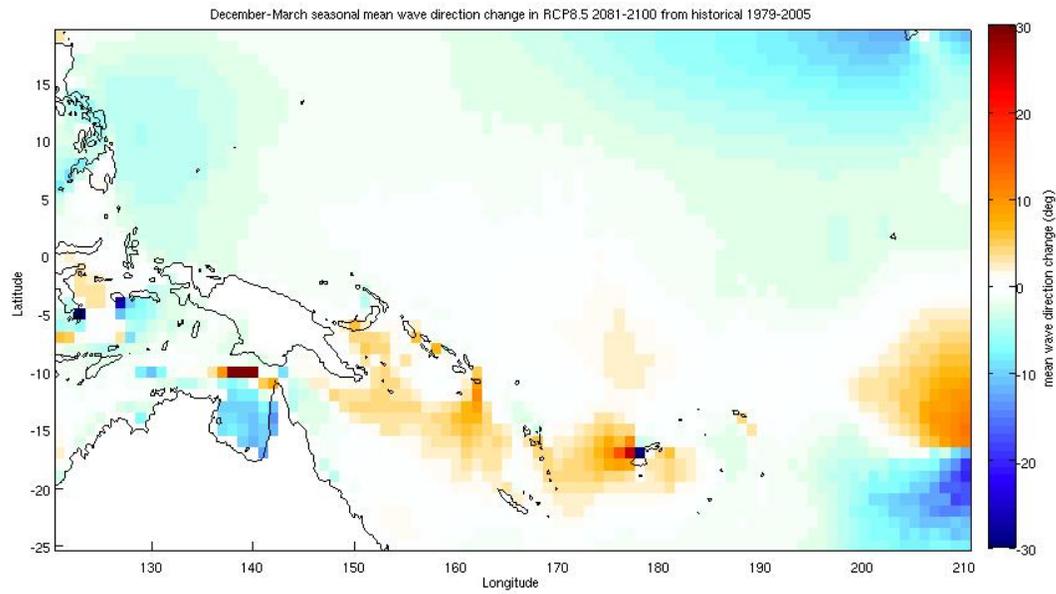
Fig. 14 December-March projected change in mean wave direction from historical (1979-2005) values in 2081-2100 under the RCP8.5 emissions scenario.
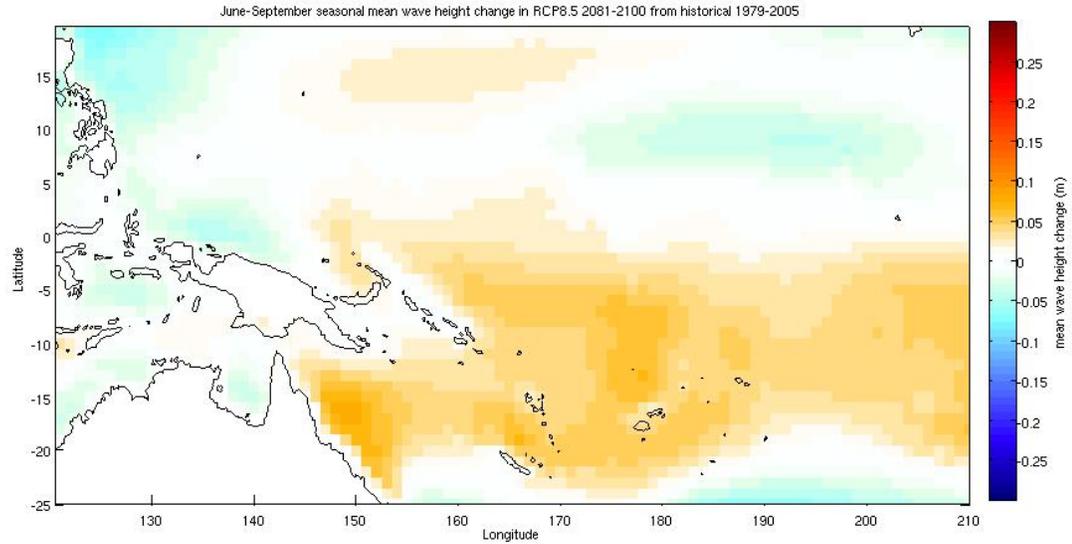
Fig. 15   June-September projected change in mean wave height from historical (1979-2005) values
in 2081-2100 under RCP8.5.
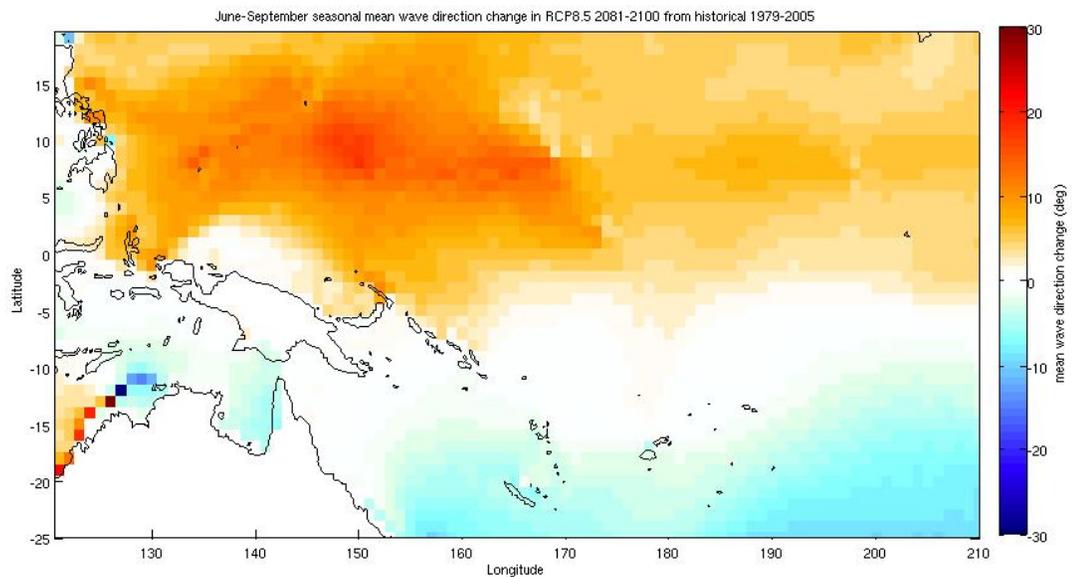
Fig. 16   June-September projected change in mean wave direction from historical (1979-2005)
values in 2081-2100 under the RCP8.5 emissions scenario.

4.1.2   Country example – Nauru

Annual cycles of the projected change signal are presented in Fig. 17, as described in Section
2.2.1. As the models were run for two different emissions scenarios and two different time
periods, four annual cycles are presented on the one set of axes. Each cycle is the monthly
average of the difference between future and historical model runs over the four climate models
used. Thus where values are negative the models for that scenario on average suggest a decrease
in parameter values from the current era; where values are positive the average of models

suggests an increase in the parameter value. Shaded boxes show 1 standard deviation of the differences between models, a large box indicates less agreement between the models, a smaller box indicates greater agreement. Error bars indicate the 5-95% range of models, assuming a normal distribution of data across the four models.
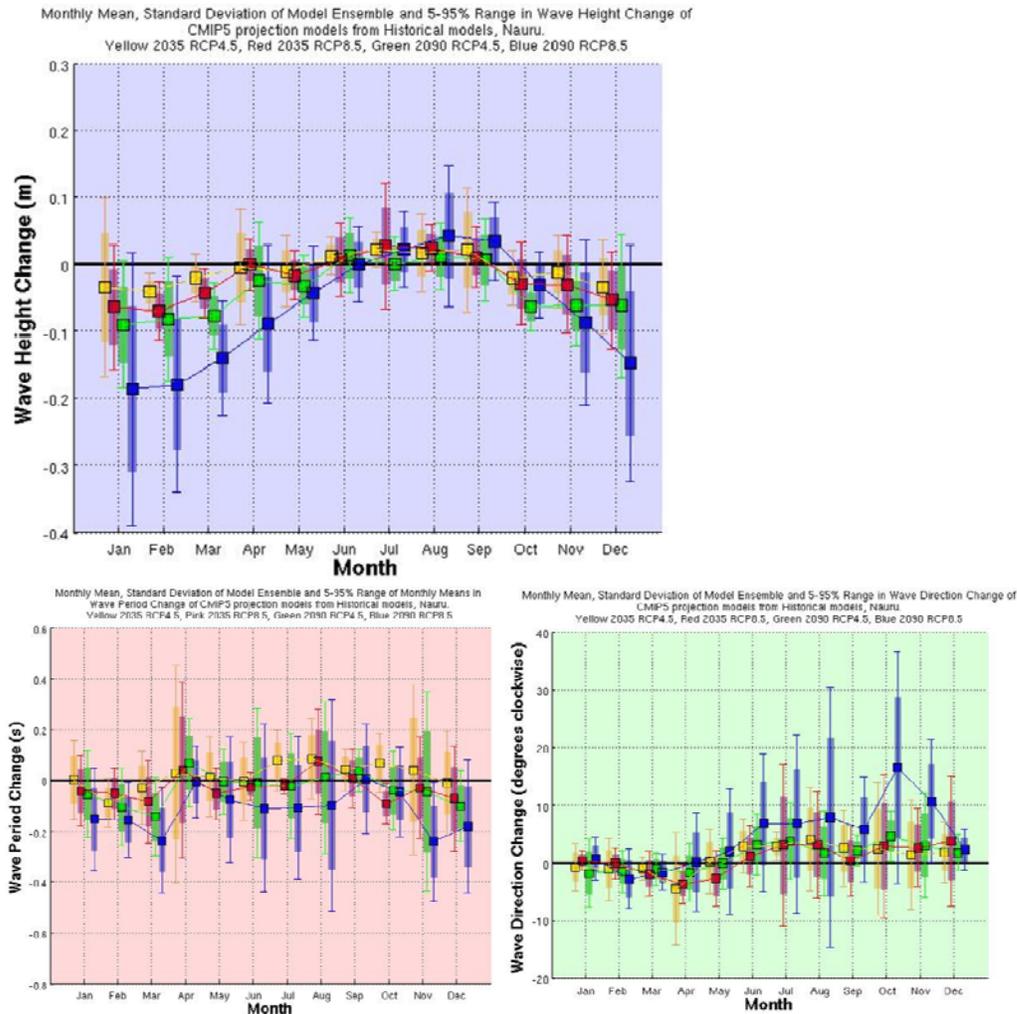
Fig. 17 **Mean annual cycles of projected change from historical values of wave height (blue background), period (red background) and direction (green background) in future time periods under RCP4.5 or RCP8.5 emissions scenarios at Nauru. Shaded boxes show 1 standard deviation of model differences and error bars show estimated 5-95% range.**

The change in wave height (top panel) shows that the projected climate model winds produce waves that are projected to be smaller in the wet season than they were historically, with this effect greater at the end of the 21st century (blue and green cycles) than in the middle of the century (yellow and red cycles), and the effect is stronger under the higher representative concentration pathway scenario RCP8.5 (red and blue cycles) than the respective lower emissions scenario RCP4.5 (yellow and green cycles). The -0.2m change in wave height (December-March) for RCP8.5 indicates a weakening of the seasonal signal, however the historical simulations have been shown to over predict the seasonal cycle compared to the hindcast by a similar amount (Section 3.2.3). This combined with consideration of other factors such as ENSO index sign and strength, and modelling method (Hemer, Fan, Mori, Semedo and

Wang, 2013) means that confidence in this change is assessed as low. No significant change is projected in wave heights at Nauru in the dry season. Note that large, not average, wave heights, should be considered when applying wave data to impact assessments.

Projected wave period changes are insignificant (lower left panel). Wave direction is projected to remain largely unchanged at Nauru (lower right panel), with a suggested clockwise rotation in the dry season (a rotation toward the south), which may be due to enhanced extra-tropical southern storms.

Seasonal summaries of the projected changes in Fig.17 are shown in Table 3.

Table 3 Projected changes in wave parameters at Nauru for December-March (wet season) and June-September (dry season). Blue numbers show RCP4.5 (low) while red numbers are for the RCP8.5 (high) scenario. The wave model was run for two twenty year periods centred on 2035 (column 3) and 2090 (column 4), subtracting the mean value from a period centred on 1995 (Table 2). The values in brackets represent the 5th to 95th percentile range of uncertainty. Column 5 gives statistical confidence in these projected values.

VARIABLE	SEASON	2035	2090	CONFIDENCE (RANGE)
Wave height change (m)	December-March	-0.0 (-0.2 – 0.2) -0.1 (-0.3 – 0.1)	-0.1 (-0.2 – 0.1) -0.2 (-0.3 – -0.1)	Low
Wave height change (m)	June-September	+0.0 (-0.1 – 0.1) +0.0 (-0.1 –0.1)	0.0 (-0.1 –0.1) +0.0 (-0.1 – 0.1)	Low
Mean wave period change (s)	December-March	-0.0(-1.1 – 1.0) -0.1 (-1.1 – 1.0)	-0.1 (-1.2 – 1.1) -0.2 (-1.3 –1.0)	Low
Mean wave period change (s)	June-September	+0.0 (-0.6 – 0.7) 0.0 (-0.6 – 0.6)	0.0 (-0.7 –0.7) -0.1 (-0.8 – 0.6)	Low
Mean wave direction change (° clockwise)	December-March	0 (-10 – 10) 0 (-10 – 10)	0 (-10 – 10) 0 (-10 – 10)	Low
Mean wave direction change (° clockwise)	June-September	+0 (-10 – 20) +0 (-10 – 20)	+0 (-10 – 20) +10 (-10 – 30)	Low

We also generate a radial probability change distribution similar to Fig.12, to analyse the projected change between historical and RCP8.5 end of century models. Figure 18 shows the change in projected distributions of mean wave period and mean wave direction between historical and end of century RCP8.5 models for the wet (left) and dry (right) seasons. In the wet season, December-March, wave period is projected to decrease while wave direction remains largely unchanged. In the dry season, waves are projected to be directed less from the east-southeast and more from the south-southeast through to west.
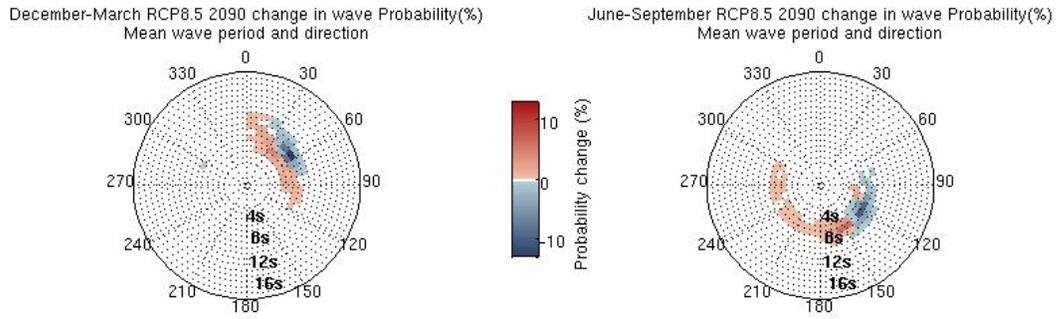
**Fig. 18** **Radial probability change density distribution for Nauru, showing mean wave period (radius) and mean wave direction (angle) in the wet season (left) and dry season (right). Colour indicates change in probability by the end of the 21st century under RCP8.5 compared to historical values. White areas may indicate no change in probability, or may contain too few data points for a significant change to be measured.**

5   RECOMMENDATIONS

The data produced and analysed in the project, PACCSAP 1.4.3 "High resolution wind-wave climate and projections of change in the Pacific region for coastal hazard assessments", has enabled us to provide modelled wave data to Pacific Island nations, with a description of their recent wave climate, and projections about how it may change over the coming century. This is an important advance in allowing the countries concerned to understand possible implications of climate change, and inform adaptation policy. The development of a high-resolution wind-wave hindcast for the Pacific region has been a major achievement of this project.

More work is required, however, to provide stakeholder groups with targeted data and information that is applicable to their immediate planning requirements. Furthermore, the datasets produced in the course of this work, particularly the high resolution wave hindcast, can provide further information such as statistical wave catalogues, which may aid understanding of wave processes.

We recommend the follow improvements and studies be undertaken:

- **Hindcast extension:** Continue to extend the wave hindcast beyond 2009, so that it will overlap with any new observational data collected in the region. Such observational data will also permit local validation of the hindcast data.

- **Increased ensemble of climate change scenarios:** Our ensemble of wave climate change scenarios is limited to 4 models. This was a result of CMIP5 data availability at the time this work was undertaken. As such, we are unable to quantify the full climate model and emission uncertainty associated with our wave climate projections. Furthermore, this study includes just one wave projection methodology. Hemer et al. (2013) suggest projection methodology is perhaps the largest source of uncertainty surrounding wave climate projections. Further work using a well-designed experiment to identify the dominant sources of variance within a larger ensemble of wave climate projections (e.g. including different climate models, scenarios and projection methodologies) is required. Reducing the uncertainties around wave projections will also contribute to improved projections of other coastal processes such as sea-level rise and storm surges.

- **Develop a regional wind-wave climatology which is easily accessible and interpretable by a broad set of stakeholders.** The information developed within this project and in the Update to Country Reports has been an essential first step towards the provision of detailed information that responds to the needs of stakeholders. However, a climatological representation of this data should be made easily available to all stakeholders, through incorporation in delivery tools under development (e.g., Climate Futures or Climate Oceans Support Program in the Pacific (COSPPac) Climate and Oceans Monitoring and Prediction (COMP) Ocean Portal)

- **Database of potential damaging swell:** Hoeke et al. (2013) identified five inundation events in the region which were a consequence of extra-tropical storm generated waves propagating into the region, resulting in coastal flooding. These events span three areas of interest in the Pacific, impacting on at least five PICs. Reported swell-driven flooding events in the Indian (Maldives) and Atlantic (Ascension) Oceans also provide examples of damaging swell events. The wave hindcast developed under this project provides a unique dataset to develop understanding of wave impacts in the region.

Following the method of (Delpey, Ardhuin, Collard and Chapron, 2010) we propose using the spectrally partitioned hindcast wave data to perform analysis to identify the source location of swells associated with the identified surge events. Surface wind and pressure fields at the time and location of the swell source should be investigated for possible links to identifiable storm systems, with statistical analysis performed to identify whether these storms were atypical or not. The hindcast record could be inspected for similar storm events and their climatological properties, and any observed responses, with statistical analyses performed to judge the likelihood and recurrence period of such events, and perhaps the seasonal likelihood of potentially damaging swell.

- **Seasonal swell prediction:** There is currently no ability to provide seasonal predictions of potential damaging swell events such as those listed above. Seasonal prediction of wave dependent flooding events, in combination with seasonal sea-level prediction, would enable preparation by communities for coastal inundation, allowing impacts to be minimised.

- **Integrated local-scale climate studies:** The hindcast provides stakeholders with up-to-date boundary conditions that can be used to drive coastal models in the region to investigate storm surge and flood risks. In the future, wave modelling should be combined with other physical processes such as sea-level change and inundation studies, as well as biogeochemistry and ecology, to understand environmental stressors in the region, and potentially to make integrated climate projections for individual islands.

GLOSSARY

CAWCR - Centre for Australian Weather and Climate Research. A research partnership between CSIRO and the Bureau of Meteorology.

CFSR - Climate Forecast System Reanalysis. Performed by NCEP. A high resolution 0.3-0.5 degree hourly reanalysis product providing the highest resolution wind dataset available at this time (Saha, et al., 2010). CFSv2, from 2011 onwards, is higher resolution but that data are not included here.

Climatology - The description and scientific study of climate. In the context of this document, we refer to a "typical" state by averaging all years of data together in each month to find the average historical January mean, February mean, etc., thus generating a standard "climatology" for wind-waves at a location, assuming no trend in the data.

CMIP3 - Coupled Model Intercomparison Project (Phase 3) is a set of climate model experiments from 17 groups in 12 countries with 24 models. Climate model output from simulations of the past, present and future climate was collected by the Program for Climate Model Diagnosis and Intercomparison (PCMDI) at Lawrence Livermore National Laboratory in the US, during 2005 and 2006. The resulting CMIP3 dataset was used to inform the Fourth Assessment Report of the Intergovernmental Panel on Climate Change. These models are now older and have lower resolutions than the current-generation CMIP5 model data. Two models from this ensemble were used to force wind-waves; ECHAM5 and CSIRO Mk3.5[4].

CMIP5 - Coupled Model Intercomparison Project (Phase 5). In September 2008, 20 climate modelling groups from around the world, agreed to develop a new set of coordinated climate model experiments to provide a wider range of emissions scenarios, and improved models and simulations for the Fifth Assessment Report of the Intergovernmental Panel on Climate Change. There are 60 models in this ensemble, but not all contain all data we may be interested in. For wind-wave modelling, only the earliest release high-resolution models with appropriate data were utilised: HadGEM2-ES, CNRM-CM5, INMCM4, and ACCESS1.04.

Direction - Mean wave direction, the mean direction of wave origin in degrees clockwise from north (bearing). Distinct from peak direction (not used in this report). See Tolman (2009).

ENSO - **El Niño - Southern Oscillation.** The term El Niño was initially used to describe a warm-water current that periodically flows along the coast of Ecuador and Peru, disrupting the local fishery. It has since become identified with a basin-wide warming of the tropical Pacific Ocean east of the dateline. This oceanic event is associated with a fluctuation of a global-scale tropical and subtropical surface pressure pattern called the Southern Oscillation. This naturally occurring coupled atmosphere-ocean phenomenon, with time scales of approximately two to seven years, is known as the El Niño-Southern Oscillation (ENSO). The state of ENSO is often measured by the Southern Oscillations Index (SOI) and sea-surface temperatures in the central and eastern equatorial Pacific.

During an ENSO event, the prevailing trade winds weaken, reducing upwelling and altering ocean currents such that the sea-surface temperatures warm, further weakening the trade winds. This event has a great impact on the wind, sea-surface temperature and precipitation patterns in

---

[4] http://cmip-pcmdi.llnl.gov/

the tropical Pacific. It has climatic effects throughout the Pacific region and in many other parts of the world. The cold phase of ENSO is called La Niña.

GCM - Global Climate Model. This is a numerical representation of the climate system based on the physical, chemical and biological properties of its components, their interactions and feedback processes, and accounting for all or some of its known properties. Coupled Atmosphere-Ocean General Circulation Models provide a representation of the climate system that is near the most comprehensive end of the spectrum currently available. There is an evolution towards more complex models with interactive chemistry and biology.

Hindcast - A statistical calculation determining probable past conditions[5]. In this case reanalysis wind data - that is wind data which has been calculated for a regular global grid based on directly and indirectly measured data on an irregular grid – is applied to a wave model to compute the likely wave structure over an historical time period, in lieu of directly sensed wave data.

Interannual - From year to year, i.e. "interannual variation" refers to usual differences in an aspect of climate between one year and the next.

ITCZ - Intertropical Convergence Zone. An east-west band of low-level wind convergence near the equator where the south-easterly trade winds of the southern hemisphere meet the north-easterly trade winds of the northern hemisphere. It is co-located with the ascending branch of the Hadley Circulation and has an associated band of heavy rainfall as the winds converge and moist air is forced upward. In this region, trade winds tend to be suppressed and thus waves are reduced.

Mid-latitude storms - Also known as "mid-latitude cyclones" or "extratropical cyclones". These weather systems develop outside the tropics, approximately in the band 30-60 degrees latitude above and below the equator. These systems are driven by strong westerly winds, forming as large low pressure systems associated with fronts, with energy coming from horizontal temperature gradients. The strongest winds in these storms are high in the atmosphere, but they can still drive very large wave systems, particularly in the Southern Ocean.

Monsoon - A monsoon refers to a seasonal reversal of wind direction. In the Western Pacific region this occurs roughly between November and April when the prevailing trade winds are replaced by moisture-laden westerly to north-westerly winds across the western portion of the Pacific basin. Monsoon winds in the region drive westerly waves, with a pronounced reduction in easterly waves.

NCEP - National Centres for Environmental Prediction. See also NCEP CFSR.

NCEP CFSR - National Centres for Environmental Prediction Climate Forecast System Reanalysis. A high resolution 0.3-0.5 degree hourly reanalysis product providing the highest resolution wind dataset available at this time (Saha, et al., 2010), as well as sea ice data. These reanalysis data were used to drive the wave hindcast produced in this study.

PACCSAP - Pacific-Australian Climate Change Science and Adaptation Programme. A collaborative research partnership between Australian Government agencies (including CSIRO and the Bureau of Meteorology), 14 Pacific Island Countries and East Timor (Timor L'este),

---

[5] From Merriam-Webster Dictionary.

and regional and international organisations. Follows on from programs previously known as PCCSP and PASAP.

Period - Mean wave period, the mean time between successive wave crests (Tolman, 2009).

Reanalysis - An analysis combining many irregular meteorological or oceanographic observations from close to the same time into a physically consistent, complete gridded data set for a given time and usually for the whole globe.

SAM - Southern Annular Mode. The Southern Annular Mode (SAM) is the most important recurring pattern of natural variability in the southern hemisphere outside of the tropics. Oscillations in the SAM are associated with shifts in the position and strength of the mid-latitude westerly winds.

SAMI - Southern Annular Mode Index. The SAMI is an index measuring the difference in surface pressure between latitudes 40°S and 65°S. A positive SAM index corresponds to a southward movement and intensification of the sub-tropical westerly winds.

Significant Wave Height - The mean height of the largest 1/3 of waves in the time interval of the model (Tolman, 2009).

SOI - Southern Oscillation Index. The southern Oscillation Index is calculated from the mouthly or seasonal fluctuation in the air pressure difference between Tahiti and Darwin. This is linked to the El Niño – Southern Oscillation, with a negative value indicating El Niño conditions.

SPCZ - South Pacific Convergence Zone. A persistent and greatly elongated zone of low-level convergence extending from approximately 140°E near the equator to approximately 120°W at 30°S. The zone is not quite linear, but is oriented more west to east near the equator and has a more diagonal orientation (northwest to southeast) at higher latitudes. In this region, winds tend to be suppressed and thus waves are reduced.

Trade Winds - The wind system occupying most of the tropics that blows from the subtropical high pressure areas toward the equator. These winds are directed from the southeast in the southern hemisphere, and from the northeast in the northern hemisphere, and produce waves with corresponding directions.

Tropical cyclone - A tropical cyclone is a tropical depression of sufficient intensity to produce sustained gale force winds (at least 63km/hr). A severe tropical cyclone produces sustained hurricane force winds (at least 118km/yr). Severe tropical cyclones correspond to the hurricanes or typhoons of other parts of the world. These systems are distinctly different in structure and nature than mid-latitude storms. In this region they are commonly associated with extreme wave events.

Wave height - See Significant Wave Height.

ACKNOWLEDGMENTS

REFERENCES

Aucan, J., Hoeke, R. and Merrifield, M. (2012). Wave-driven sea level anomalies at the Midway tide gauge as an index of North Pacific storminess over the past 60 years. *Geophysical Research Letters , 39* (17).

Bidlot, J., Janssen, P. and Abdalla, S. (2005). A revised formulation for ocean wave dissipation in CY29R1. *ECMWF* Technical memorandum *, R60.9/JB/0(1)*, pp. 1-35.

Church, J., White, N. and Hunter, J. (2006). Sea-level rise at tropical Pacific and Indian Ocean islands. *Global and Planetary Change , 53* (3), 155-168.

Dee, D., Uppala, S., Simmons, A., Berrisford, P., Poli, P., Kobayashi, S., et al. (2011). The ERA-Interim reanalysis: configuration and performance of the data assimilation system. *Quarterly Journal of the Royal Meteorological Society , 137* (656).

Delpey, M., Ardhuin, F., Collard, F. and Chapron, B. (2010). Space-time structure of long ocean swell fields. *J. Geophys. Res. , 115* (C12037).

Dobrynin, M., Murawsky, J. and Yang, S. (2012). Evolution of the global wind wave climate in CMIP5 experiments. *Geophysical Research Letters , 39* (L18606).

Durrant, T., Greenslade, D., Hemer, M. and Trenham, C. (In prep). A global wave hindcast focussed on the South Pacific. CAWCR Technical Report .

Durrant, T., Hemer, M., Trenham, C. and Greenslade, D. (2013). CAWCR wave hindcast 1979-2010 v4. Retrieved from http://dx.doi.org/10.4225/08/523168703DCC5.

Fan, Y., Held, I. and Lin, S.-J. (2013). Ocean warming effect on Surface Gravity Wave Climate Change for the end of the 21st Century. *Journal of Climate* , e-view.

Grose, M., Brown, J., Narsey, S., Brown, J., Murphy, B., Langlais, C., et al. (accepted). Assessment of the CMIP5 global climate model simulations of the western tropical Pacific climate system and comparison to CMIP3. *International Journal of Climatology.*

Guilyardi, E., Wittenberg, A., Federov, A., Collins, M., Wang, C., Capotondi, A., et al. (2009). Understanding El Niño in ocean-atmosphere general circulation models: Progress and challenges. *BAMS* , 325-340.

Hanson, J. and Phillips, O. (2001). Automated analysis of ocean surface directional wave spectra. *Journal of atmospheric and oceanic technology , 18*, 277-293.

Hanson, J., Tracy, B., Tolman, H. and Scott, R. (2009). Pacific Hindcast Performance of Three Numerical Wave Models. *J. Atmos. Oceanic Technol. , 26*, 1614-1633.

Harangozo, S. (1992). Flooding in the Maldives and its implications for the global sea level rise debate. In P. Woodworth, D. Pugh, J. DeRonde, R. Warrick and J. Hannah (Eds.), *Sea Level Changes: Determination and Effects* (Vols. Geographical Monograph Series 69, 196, pp. 95-99). Washington DC: AGU.

Hemer, M., Fan, Y., Mori, N., Semedo, A. and Wang, X. (2013). Projected future changes in wind-wave climate in a multi-model ensemble. *Nature*.

Hemer, M., Katzfey, J. and Hotan, C. (2011). The wind-wave climate of the Pacific Ocean, PASAP final report. Canberra: DCCEE.

Hemer, M., Katzfey, J. and Trenham, C. (2013). Global dynamical projections of surface ocean wave climate for a future high greenhouse gas emission scenario. *Ocean Modelling , 70*, 221-245.

Hemer, M., Wang, X., Weisse, R. and Swail, V. (2012). Advancing Wind-Waves Climate Science: The COWCLIP Project. *Bulletin of the American Meteorological Society , 93*, 791-796.

Hoeke, R., McInnes, K., Kruger, J., McNaught, R., Hunter, J. and Smithers, S. (2013). Widespread inundation of Pacific islands by distant-source wind-waves. *Global and Planetary Change , 108*, 128-138.

Knutson, T., McBride, J., Chan, J., Emanuel, K., Holland, G., Landsea, C., et al. (2010). Tropical cyclones and climate change. *Nature Geoscience , 3*, 157-163.

Lavender, S. and Walsh, K. (2011). Dynamically downscaled simulations of Australian region tropical cyclones in current and future climates. *Geophysical Research Letters , 38* (10).

Mori, N., Shimura, T., Yasuda, T. and Mase, H. (2013). Multi-model climate projections of ocean surface variables under different climate scenarios - Future changes of waves, sea level and wind. *Ocean Engineering , 71*, 122-129.

Nicholls, R., Wong, P., Burkett, V., Codignotto, J., Hay, J., McLean, R., et al. (2007). Coastal systems and low-lying areas. In M. Parry, O. Canziana, J. Palutikof, P. van der Linden, C. Hanson. and Eds., *Climate Change 2007: Imacts, Adaptation and Vulnerability.* Contribution to Working Group II to the Fourth Assessment Report of the Intergovernmental Panel on Climate Change (pp. 315-356). Cambridge, UK: Cambridge University Press.

Saha, S., Moorthi, S., Pan, H., Wu, X., Wang, J., Nadiga, S., et al. (2010). The NCEP climate forecast system reanalysis. *Bulletin of the American Meteorological Society , 91* (8), 1015-1057.

Semedo, A., Weisse, R., Behrens, A., Sterl, A., Bengtsson, L. and Günther, H. (2013). Projection of global wave climate change towards the end of the 21st century. *Journal of Climate* , e-view.

Tolman, H. (2008). A mosaic approach to wind wave modeling. *Ocean Modelling , 25* (1-2), 35-47.

Tolman, H. (1991). A Third-Generation Model for Wind Waves on Slowly Varying, Unstead, and Inhomogeneous Depths and Currents. *Journal of Physical Oceanography , 21* (6), 782-797.

Tolman, H. (2009). User manual and system documentation of WaveWatch III TM version 3.14. NOAA/NWS/NCEP/MMAB.

van Vuuren, D., Edmonds, J., Kainuma, M., Riahi, K. and Weyant, J. (2011). The representative concentration pathways: an overview. *Climatic Change , 109* (1-2).

Walsh, K., McInnes, K. and McBride, J. (2012). Climate change impacts on tropical cyclones and extreme sea levels in the South Pacific - A regional assessment. *Global and Planetary Change , 80-81*, 149-164.

Young, I., Zieger, S. and Babanin, A. (2011). Global Trends in Wind Speed and Wave Height. *Science , 332* (6028), 451-455.

Zhang, X. and Church, J. (2012). Sea level trends, interannual and decadal variability in the Pacific Ocean. *Geophysical Research Letters , 39* (21).